# Lab 3: Airfoil Design and Test

Unified Engineering

Andrew Kurtz, Edward Lopez, Andrew Trattner, and Lisa Yang

April 10th, 2015

## Contents

# 1 Description

The goal of this lab is to test the actual performance of a symmetric and a cambered airfoil in a 1x1 ft wind tunnel to determine net lift and drag forces. To accomplish this, the team will first determine the wind tunnel conditions and length of the chord to achieve dynamic similarity with an RC aircraft with a chord of 7 inches and a speed of 30 mph. The test results will be compared to XFOIL data, and discrepancies will be explained. This lab uses concepts learned in Unified and demonstrates the difficulty in performing experiments to quantify certain aerodynamic measurements in two-dimensional flow. The team will use what is learned in this lab to assist in the designing of the airfoil in the upcoming Unified Engineering Flight Competition.

# 2 Results and Analysis

## 2.1 Drag and Lift Calculations Using Load Cell

The average values of force $f'$ for each angle of attack $\alpha$ in the data sheet may be manipulated to find $C_L$ and $C_D$. This analysis assumes the calibration matrix and other considerations, such as zeroing the readings by subtracting the stand's effect on the force sensor, have already been applied to the data.

1. Combine the forces using trigonometry to normalize the axes. $\hat{x}$ points along the chord in the tail direction, $\hat{y}$ points in the vertical lift direction.

$$f_x = f_{channel2=y'} \sin(\alpha) + f_{channel1=x'} \cos(\alpha)$$
$$f_y = f_{channel2=y'} \cos(\alpha) - f_{channel1=x'} \sin(\alpha)$$

2. Since the drag and lift forces are $\frac{1}{2}\rho v^2 C S_{ref}$ and are equal to $f_x$, $f_y$ respectively:

$$C_D = \frac{f_x}{\frac{1}{2}\rho v^2 S_{ref}} \qquad C_L = \frac{f_y}{\frac{1}{2}\rho v^2 S_{ref}}$$

3. Plot these coefficients for each angle of attack and airfoil. Velocity tested on average is $42mph = 18.8\frac{m}{s}$ and $S_{ref} = 0.039m^2$. Density is assumed to be standard sea level value of $1.225\frac{kg}{m^3}$.

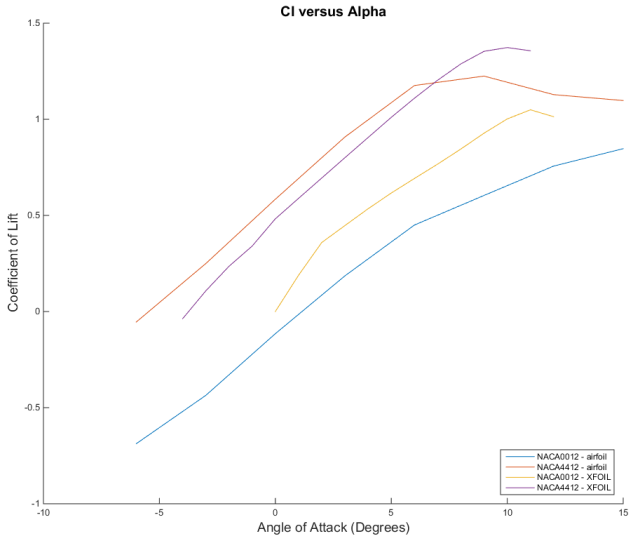


Figure 1: $C_L$ versus $\alpha$

Experimental values appear to follow the trends given by the XFOIL data. The NACA 0012 symmetric airfoil performed slightly worse than the XFOIL simulation, with the lift coefficient approximately

0.2 less than that of XFOIL on average. The NACA 4412 cambered airfoil surpassed the XFOIL simulation by approximately 0.1 on average, until the angle of attack reaches 5 degrees, at which point the experiment undershoots the prediction given by XFOIL.

What would cause a cambered airfoil to outperform XFOIL, while a symmetric one underperforms? Because the experimental setup did not allow for testing of the load cell lever arm's contribution to the forces in windy conditions without a wing attached, the degree to which proper calibration affects the results is unknown. For small discrepancies, such as the 4412 versus XFOIL for $\alpha < 5$, the calibration may be the sole factor. In addition, small imperfections along the trailing edge were noted for both airfoils. Though these are negligible, they contribute in part to the underperformance seen for both wings at high angles of attack, since some of the planform surface is simply gone, so the pressure differential which causes lift to rise at high angles of attack is not able act as effectively on the wing and translate to the load cell. Other manufacturing imperfections may be invisible but present, increasing drag and obstructing lift through marginally increased boundary layer thickness. It is also possible that the speed of the wind tunnel was imprecisely tuned to create the dynamic similarity desired. With the available instrumentation, the wind tunnel was operated as accurately as possible, but even so perturbations in the flow caused the speed readings to fluctuate throughout the trials. Though the average over 10 seconds of data should ideally filter out this noise, it is conceivable that the load cell becomes less accurate over time in these conditions. Most significantly, as the wings were constructed of foam, the entire lift force may simply not have all translated to the load cell through the lever arm. In particular, the symmetric airfoil noticeably vibrated on the stand, indicating that the flexing of the wings may have failed to translate completely and accurately to the sensor, causing it to read less than what XFOIL's idealization provides.

In Figure 2, the trends for drag polars are quite clear. The symmetric 0012 airfoil yields a particularly round drag polar, exactly as expected. However, the curve is shifted right by 0.02 on average, with more drag measured than XFOIL predicts.

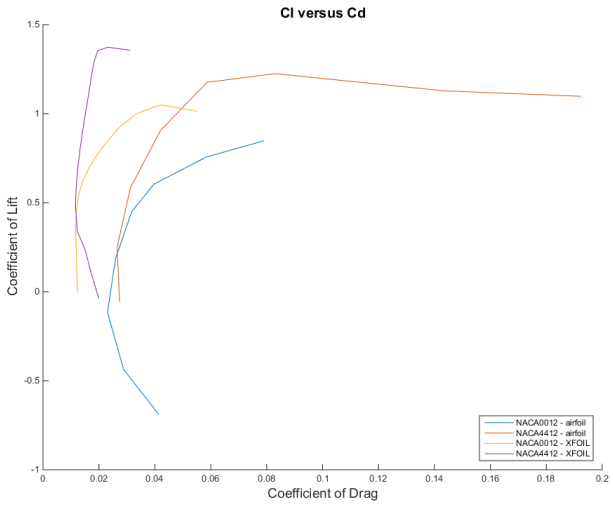


Figure 2: $C_L$ versus $C_D$

Additional drag is expected, since as stated previously, no calibration tests for an empty stand in windy conditions were recorded. So even though the resting weight of the airfoil and forces at various angles of attack were factored into the calculation from sensor voltages to forces, drag due to the stand in test conditions was not accounted for. Although the discrepancy at some points is over twofold for both airfoil curves, the absolute difference between the experimental and predicted drag coefficient is no more than 0.05 for all except the most extreme angles of attack. This relatively large but actually fairly small amount (considering the magnitude of lift coefficient) may be accounted for by the imperfections in the wings, the inadequate calibration, wind tunnel turbulence and speed variation, and small load cell inaccuracies at the small voltage resolution required to measure drag.

## 2.2 Drag Calculations Using Momentum Deficit

Drag of the airfoil can also be determined by calculating the momentum deficit in the wake produced by the airfoil. It is assumed that the flow is identical at each spanwise location and using the nearfield wake, $\Theta_\infty$ is the momentum thickness of the field wake:

$$\Theta_\infty \approx \Theta = span \cdot \int (1 - \frac{u}{V_\infty}) \frac{u}{V_\infty} dz \tag{1}$$

In the above equation, $\frac{u}{V_\infty}$ is defined as:

$$\frac{u}{V_\infty} = \sqrt{\frac{h_{0i} - h_\infty}{h_{0\infty} - h_\infty}}$$

where:

$h_\infty$ = average height of columns 1 and 25 of liquid which correspond to static ports

$h_{0\infty}$ = average height of columnds 2 and 24 of liquid which correspond to stagnation ports at infinity

$h_{0i}$ = height of each column from i = 3 to 23 which correspond to stagnation ports

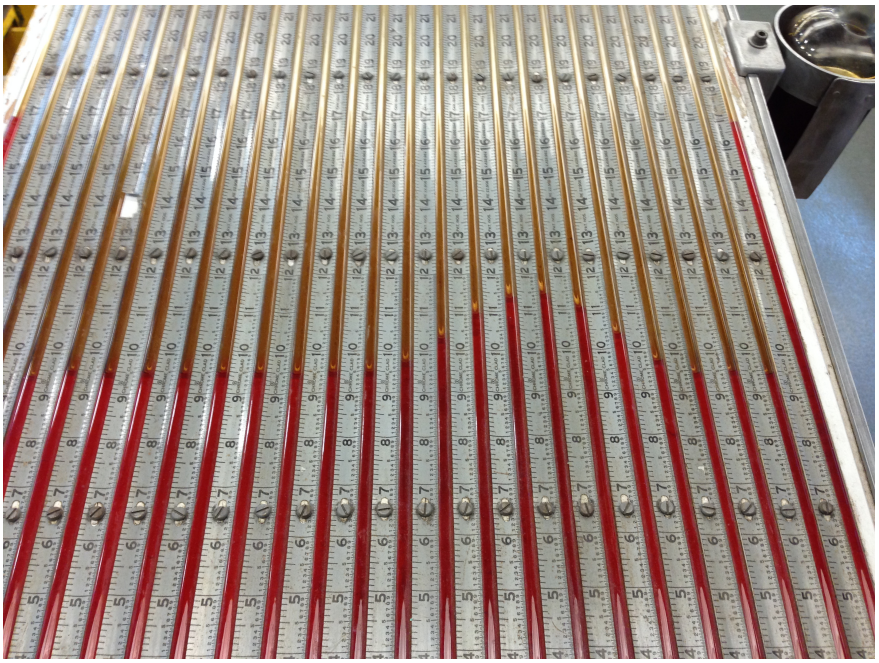

Figure 3: Monometer Rig

Using a summation instead of an integral to calculate the momentum thickness $\Theta$:

$$\Theta = span(1 - \frac{u}{V_\infty}) \frac{u}{V_\infty} * h \tag{2}$$

where h is the spacing between the pitot tubes. For $\alpha$ = -6, -3, 0, 3, 6, $h = \frac{sqrt2}{2} 0.15in \approx 2.69 \times 10^{-3} m$.

Initially, the tests were conducted with the pitot array vertically oriented. It was then found that a 45 degree incline provides better resolution for calculating drag. A comparison of the two orientations is found overleaf.

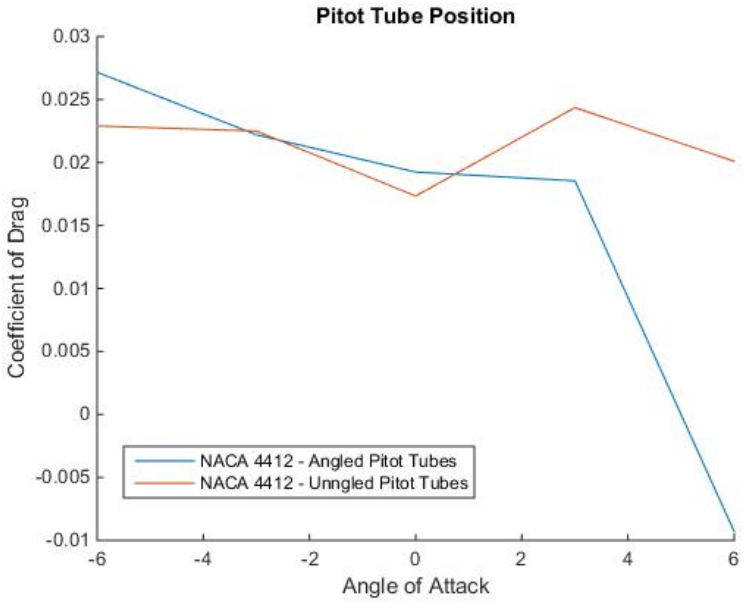


Figure 4: Low and High Sensitivity Pitot Tube Error

In Figure 4, both drag coefficients decrease as they approach 0 angle of attack, as expected. The finer resolution of the angled pitot tubes more clearly demonstrates this trend, since the vertical tube array is unable to detect differences between angles -3 and -6, for instance. After 0 angle of attack, the angled array loses fidelity since the range is too small to detect when the flow is turned past a certain point by the airfoil. Future experiments should repeat this testing and further characterize the improvements and drawbacks of using an angled array. These results suggest that the angled array is superior, given that the experimental setup is designed to ensure continuous readings. This experiment demonstrates the effects of failure to fully capture the momentum deficit given the array's small range. Further analysis shows this trend more clearly.

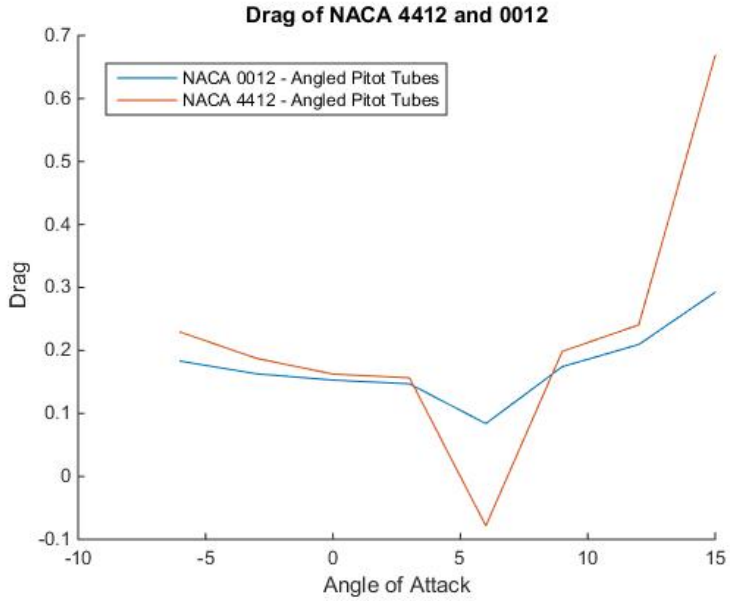


Figure 5: High-Sensitivity Drag

For instance, in Figure 5 when both airfoils are tested using the angled configuration for enhanced accuracy, the 6 degree angle of attack clearly demonstrates an apparent cusp discontinuity, at which point the angled pitot tube array is reverted back to vertical for the 9 degree test as protocol and TA suggests. The most extreme case for the angled array is 6 degrees, and these results suggest that unless the rig is translated vertically, the angled array is not ideal for capturing momentum deficit past 3 degrees.

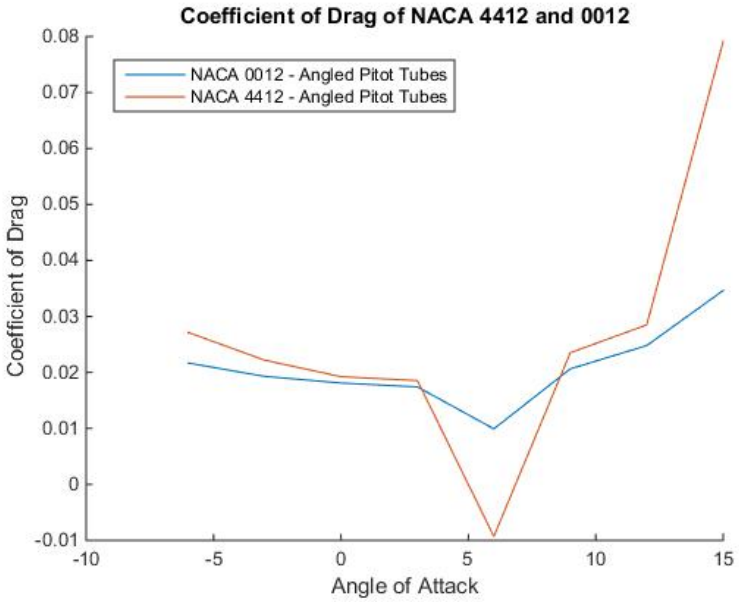


Figure 6: High-Sensitivity Drag Coefficient

Despite the distortion caused by the pitot array's improper alignment, referring back to Figure 2 shows that the drag created by the wing as calculated through momentum deficit is more accurate in non pitot-limited cases than the load cell sensor readings. For example, at 0 degree angle of attack, the NACA 0012 airfoil generates a drag coefficient of 0.02 via momentum deficit, whereas the drag coefficient according to the load cell is 0.03. This difference, as stated previously, is likely due to the lever arm of the sensor. It is reasonable that the pitot did not pick up on this additional source of drag since it is centered on the wing and for this experiment was located off-center exactly so as to not be affected by disturbances caused due to the lever arm. These results reinforce the analysis earlier as to why the curves are offset from the XFOIL data. Future experiments should characterize the behavior of the test stand without an airfoil in wind test conditions to verify this result.

# 3 Error

Kurtzy

# 4 Conclusion

Kurtzy

# 5 Data Sheets

Windtunnel Data

NACA0012

| Alpha | -6 | -3 | 0 | 3 | 6 | 9 | 12 | 15 |
|---|---|---|---|---|---|---|---|---|
| Baseline average V_x | -0.1008 | -0.0845 | -0.0679 | -0.05 | -0.0354 | -0.0186 | -0.0033 | 0.0123 |
| Experiment average V_x | -0.0637 | -0.0174 | -0.0151 | -0.0592 | -0.1469 | -0.2133 | -0.1777 | -0.1798 |
| Actual V_x | 0.0371 | 0.0671 | 0.0528 | -0.0093 | -0.1115 | -0.1947 | -0.1744 | -0.1921 |
| F_x | 0.1855 | 0.3355 | 0.2641 | -0.0464 | -0.5575 | -0.9735 | -0.8722 | -0.9604 |
| Drag | 0.2311 | 0.2237 | 0.2641 | 0.3555 | 0.4952 | 0.7005 | 1.2104 | 1.6222 |
| Coefficient of Drag | 0.0274 | 0.0265 | 0.0313 | 0.0421 | 0.0586 | 0.083 | 0.1434 | 0.1921 |
| | | | | | | | | |
| Baseline average V_y | -0.0373 | -0.0387 | -0.0395 | -0.0391 | -0.0386 | -0.0369 | -0.0345 | -0.0311 |
| Experiment average V_y | -0.1326 | 0.4156 | 1.0145 | 1.6015 | 2.1069 | 2.2333 | 2.0862 | 2.074 |
| Actual V_y | -0.0953 | 0.4543 | 1.054 | 1.6405 | 2.1455 | 2.2702 | 2.1207 | 2.1051 |
| F_y | -0.4458 | 2.1264 | 4.9328 | 7.6776 | 10.041 | 10.6245 | 9.9249 | 9.8518 |
| Lift | -0.4627 | 2.1059 | 4.9328 | 7.6647 | 9.9277 | 10.3414 | 9.5267 | 9.2675 |
| Coefficient of Lift | -0.0548 | 0.2494 | 0.5843 | 0.9078 | 1.1759 | 1.2249 | 1.1284 | 1.0977 |

NACA4412

| Alpha | -6 | -3 | 0 | 3 | 6 | 9 | 12 | 15 |
|---|---|---|---|---|---|---|---|---|
| Baseline average V_x | -0.10068 | -0.08395 | -0.06737 | -0.0522 | -0.03558 | -0.01897 | -0.00397 | 0.012283 |
| Experiment average V_x | -0.15384 | -0.07386 | -0.02844 | -0.0247 | -0.06234 | -0.11718 | -0.1891 | -0.2666 |
| Actual V_x | -0.05317 | 0.010085 | 0.038925 | 0.027498 | -0.02676 | -0.09821 | -0.18513 | -0.27888 |
| F_x | -0.26583 | 0.050423 | 0.194626 | 0.13749 | -0.1338 | -0.49103 | -0.92564 | -1.39441 |
| Drag | 0.348831 | 0.243277 | 0.194626 | 0.219006 | 0.267825 | 0.334856 | 0.493315 | 0.666259 |
| Coefficient of Drag | 0.0413 | 0.0288 | 0.0231 | 0.0259 | 0.0317 | 0.0397 | 0.0584 | 0.0789 |
| | | | | | | | | |
| Baseline average V_y | -0.04394 | -0.04427 | -0.04526 | -0.04449 | -0.04338 | -0.04162 | -0.0392 | -0.03605 |
| Experiment average V_y | -1.29745 | -0.83193 | -0.25316 | 0.28909 | 0.776116 | 1.078208 | 1.398302 | 1.625967 |
| Actual V_y | -1.25351 | -0.78766 | -0.2079 | 0.333583 | 0.819496 | 1.119825 | 1.437506 | 1.662018 |
| F_y | -5.86642 | -3.68624 | -0.97298 | 1.561168 | 3.835243 | 5.240781 | 6.727526 | 7.778242 |
| Lift | -5.8065 | -3.68383 | -0.97298 | 1.566225 | 3.800247 | 5.099444 | 6.388061 | 7.152305 |
| Coefficient of Lift | -0.6877 | -0.4363 | -0.1152 | 0.1855 | 0.4501 | 0.604 | 0.7566 | 0.8471 |

Monometer Readings

| Port | NACA 4412 | | | | | | | | NACA 0012 | | | | | | | | NACA 4412 (with angle) | | | | |
|---|---|---|---|---|---|---|---|---|---|---|---|---|---|---|---|---|---|---|---|---|---|
| | angle = -6 | angle = -3 | angle = 0 | angle = 3 | angle = 6 | angle = 9 | angle = 12 | angle = 15 | angle = -6 | angle = -3 | angle = 0 | angle = 3 | angle = 6 | angle = 9 | angle = 12 | angle = 15 | angle = -6 | angle = -3 | angle = 0 | angle = 3 | angle = 6 |
| 1 | 17 | 17 | 17 | 17 | 17 | 17 | 17 | 16.5 | 17 | 17 | 17 | 16.9 | 16.8 | 17 | 16.9 | 16.8 | 16.8 | 16.8 | 16.9 | 16.9 | 16.9 |
| 2 | 9.4 | 9.4 | 9.5 | 9.4 | 9.4 | 9.4 | 9.3 | 9 | 9.4 | 9.4 | 9.4 | 9.4 | 9.4 | 9.4 | 9.4 | 9.3 | 9.4 | 9.4 | 9.4 | 9.4 | 9.4 |
| 3 | 9.4 | 9.5 | 9.5 | 9.5 | 9.5 | 9.4 | 9.4 | 9.1 | 9.4 | 9.5 | 9.5 | 9.5 | 9.5 | 9.4 | 9.4 | 9.4 | 9.4 | 9.4 | 9.4 | 9.4 | 9.4 |
| 4 | 9.4 | 9.4 | 9.5 | 9.5 | 9.4 | 9.6 | 9.4 | 9.1 | 9.4 | 9.4 | 9.4 | 9.6 | 9.7 | 9.4 | 9.4 | 9.7 | 9.4 | 9.4 | 9.5 | 9.4 | 9.4 |
| 5 | 9.4 | 9.5 | 9.5 | 9.6 | 9.5 | 10.1 | 9.6 | 9.3 | 9.5 | 9.5 | 9.5 | 10 | 9.8 | 9.5 | 9.7 | 10.5 | 9.5 | 9.5 | 9.5 | 9.5 | 9.5 |
| 6 | 9.4 | 9.4 | 9.5 | 9.5 | 9.5 | 10.4 | 9.7 | 9.4 | 9.5 | 9.4 | 9.5 | 10.2 | 10.3 | 9.6 | 10.1 | 11.1 | 9.4 | 9.4 | 9.4 | 9.4 | 9.5 |
| 7 | 9.4 | 9.4 | 9.5 | 9.6 | 10 | 10.7 | 10 | 9.8 | 9.4 | 9.5 | 9.7 | 10.4 | 10.6 | 10 | 11 | 11.5 | 9.5 | 9.4 | 9.4 | 9.4 | 9.7 |
| 8 | 9.4 | 9.4 | 9.5 | 9.6 | 10.4 | 10.5 | 10.3 | 10.2 | 9.5 | 9.5 | 10 | 10.3 | 10.4 | 10.7 | 11.3 | 11.2 | 9.4 | 9.4 | 9.4 | 9.4 | 10.1 |
| 9 | 9.6 | 9.4 | 9.5 | 9.9 | 10.7 | 10.2 | 10.6 | 10.8 | 9.4 | 9.5 | 10.4 | 10.3 | 10.1 | 11.1 | 10.9 | 10.4 | 9.4 | 9.4 | 9.4 | 9.6 | 10.7 |
| 10 | 10.5 | 9.4 | 9.6 | 10.4 | 10.5 | 10 | 10.6 | 11 | 9.4 | 9.7 | 10.4 | 10 | 9.8 | 10.5 | 10 | 9.7 | 9.5 | 9.4 | 9.4 | 10 | 10.9 |
| 11 | 11.3 | 9.7 | 10 | 10.7 | 10 | 9.8 | 10.4 | 11.2 | 9.5 | 10.2 | 10.3 | 9.9 | 9.6 | 9.8 | 9.5 | 9.4 | 9.5 | 9.4 | 9.5 | 10.5 | 10.8 |
| 12 | 11.3 | 10.2 | 10.5 | 10.6 | 9.8 | 9.5 | 10.1 | 11.5 | 10 | 10.5 | 10.1 | 9.7 | 9.5 | 9.5 | 9.4 | 9.4 | 9.5 | 9.5 | 10 | 10.8 | 10.4 |
| 13 | 10.4 | 11 | 10.7 | 10.1 | 9.4 | 9.4 | 9.7 | 11.3 | 10.6 | 10.7 | 10 | 9.5 | 9.4 | 9.4 | 9.4 | 9.4 | 9.5 | 9.7 | 10.6 | 10.7 | 10 |
| 14 | 9.6 | 11 | 10.4 | 9.7 | 9.4 | 9.4 | 9.5 | 11.1 | 11.1 | 10.6 | 9.9 | 9.5 | 9.4 | 9.4 | 9.4 | 9.4 | 9.7 | 10.3 | 11 | 10.5 | 0.7 |
| 15 | 9.4 | 10.4 | 10 | 9.6 | 9.4 | 9.4 | 9.4 | 10.7 | 11 | 10.4 | 9.8 | 9.5 | 9.5 | 9.4 | 9.4 | 9.4 | 10.3 | 11 | 10.9 | 10 | 9.6 |
| 16 | 9.4 | 9.9 | 9.7 | 9.5 | 9.4 | 9.4 | 9.4 | 10.5 | 10.7 | 10 | 9.6 | 9.5 | 9.5 | 9.4 | 9.4 | 9.4 | 10.9 | 11.4 | 10.5 | 9.7 | 9.5 |
| 17 | 9.4 | 9.4 | 9.4 | 9.5 | 9.4 | 9.4 | 9.4 | 10 | 10 | 9.7 | 9.5 | 9.4 | 9.5 | 9.4 | 9.3 | 9.3 | 11.3 | 11.1 | 10 | 9.5 | 9.4 |
| 18 | 9.4 | 9.4 | 9.4 | 9.5 | 9.4 | 9.4 | 9.4 | 9.8 | 9.6 | 9.5 | 9.5 | 9.5 | 9.5 | 9.4 | 9.4 | 9.4 | 11.4 | 10.5 | 9.6 | 9.5 | 9.4 |
| 19 | 9.4 | 9.4 | 9.4 | 9.4 | 9.4 | 9.4 | 9.4 | 9.4 | 9.4 | 9.4 | 9.4 | 9.4 | 9.5 | 9.4 | 9.4 | 9.4 | 11 | 9.8 | 9.5 | 9.4 | 9.4 |
| 20 | 9.4 | 9.4 | 9.3 | 9.4 | 9.4 | 9.4 | 9.4 | 9.2 | 9.3 | 9.4 | 9.4 | 9.4 | 9.5 | 9.4 | 9.4 | 9.4 | 10.4 | 9.5 | 9.4 | 9.4 | 9.4 |
| 21 | 9.4 | 9.4 | 9.3 | 9.4 | 9.4 | 9.4 | 9.4 | 9.1 | 9.3 | 9.4 | 9.4 | 9.4 | 9.6 | 9.4 | 9.4 | 9.4 | 9.7 | 9.4 | 9.4 | 9.4 | 9.4 |
| 22 | 9.3 | 9.4 | 9.4 | 9.4 | 9.4 | 9.4 | 9.4 | 9 | 9.3 | 9.4 | 9.4 | 9.4 | 9.7 | 9.4 | 9.4 | 9.4 | 9.4 | 9.4 | 9.4 | 9.4 | 9.4 |
| 23 | 9.4 | 9.4 | 9.4 | 9.4 | 9.4 | 9.4 | 9.4 | 9 | 9.3 | 9.4 | 9.4 | 9.4 | 9.7 | 9.4 | 9.4 | 9.4 | 9.4 | 9.4 | 9.4 | 9.4 | 9.4 |
| 24 | 9.4 | 9.4 | 9.4 | 9.4 | 9.4 | 9.4 | 9.4 | 9 | 9.3 | 9.4 | 9.4 | 9.4 | 9.7 | 9.4 | 9.4 | 9.4 | 9.4 | 9.4 | 9.4 | 9.4 | 9.4 |
| 25 | 17 | 17 | 17 | 17 | 17 | 17 | 17 | 16.6 | 17 | 17 | 17 | 17 | 16.9 | 17 | 16.9 | 16.9 | 16.8 | 16.9 | 17 | 17 | 17 |

Note: The camera angle in NACA 4412 (angle = -6) was different from all the other images. This affected numbers. Very difficult to see the numbers; did the best to estimate accurately.

| NACA 4412 | | | | | | | | NACA 0012 | | | | | | | | NACA 4412 (with angle) | | | | |
|---|---|---|---|---|---|---|---|---|---|---|---|---|---|---|---|---|---|---|---|---|
| angle = -6 | angle = -3 | angle = 0 | angle = 3 | angle = 6 | angle = 9 | angle = 12 | angle = 15 | angle = 9 | angle = 12 | angle = 15 | angle = -6 | angle = -3 | angle = 0 | angle = 3 | angle = 6 | angle = -6 | angle = -3 | angle = 0 | angle = 3 | angle = 6 |
| 17 | 17 | 17 | 17 | 17 | 17 | 17 | 16.5 | 17 | 16.9 | 16.8 | 17 | 17 | 17 | 16.9 | 16.8 | 16.8 | 16.8 | 16.9 | 16.9 | 16.9 |
| 9.4 | 9.4 | 9.5 | 9.4 | 9.4 | 9.4 | 9.3 | 9 | 9.4 | 9.4 | 9.3 | 9.4 | 9.4 | 9.4 | 9.4 | 9.4 | 9.4 | 9.4 | 9.4 | 9.4 | 9.4 |
| 9.4 | 9.5 | 9.5 | 9.5 | 9.5 | 9.4 | 9.4 | 9.1 | 9.4 | 9.4 | 9.4 | 9.4 | 9.5 | 9.5 | 9.5 | 9.5 | 9.4 | 9.4 | 9.4 | 9.4 | 9.4 |
| 9.4 | 9.4 | 9.5 | 9.5 | 9.4 | 9.6 | 9.4 | 9.1 | 9.4 | 9.4 | 9.7 | 9.4 | 9.4 | 9.4 | 9.6 | 9.7 | 9.4 | 9.4 | 9.5 | 9.4 | 9.4 |
| 9.4 | 9.5 | 9.5 | 9.6 | 9.5 | 10.1 | 9.6 | 9.3 | 9.5 | 9.7 | 10.5 | 9.5 | 9.5 | 9.5 | 10 | 9.8 | 9.5 | 9.5 | 9.5 | 9.5 | 9.5 |
| 9.4 | 9.4 | 9.5 | 9.5 | 9.5 | 10.4 | 9.7 | 9.4 | 9.6 | 10.1 | 11.1 | 9.5 | 9.4 | 9.5 | 10.2 | 10.3 | 9.4 | 9.4 | 9.4 | 9.4 | 9.5 |
| 9.4 | 9.4 | 9.5 | 9.6 | 10 | 10.7 | 10 | 9.8 | 10 | 11 | 11.5 | 9.4 | 9.5 | 9.7 | 10.4 | 10.6 | 9.5 | 9.4 | 9.4 | 9.4 | 9.7 |
| 9.4 | 9.4 | 9.5 | 9.6 | 10.4 | 10.5 | 10.3 | 10.2 | 10.7 | 11.3 | 11.2 | 9.5 | 9.5 | 10 | 10.3 | 10.4 | 9.4 | 9.4 | 9.4 | 9.4 | 10.1 |
| 9.6 | 9.4 | 9.5 | 9.9 | 10.7 | 10.2 | 10.6 | 10.8 | 11.1 | 10.9 | 10.4 | 9.4 | 9.5 | 10.4 | 10.3 | 10.1 | 9.4 | 9.4 | 9.4 | 9.6 | 10.7 |
| 10.5 | 9.4 | 9.6 | 10.4 | 10.5 | 10 | 10.6 | 11 | 10.5 | 10 | 9.7 | 9.4 | 9.7 | 10.4 | 10 | 9.8 | 9.5 | 9.4 | 9.4 | 10 | 10.9 |
| 11.3 | 9.7 | 10 | 10.7 | 10 | 9.8 | 10.4 | 11.2 | 9.8 | 9.5 | 9.4 | 9.5 | 10.2 | 10.3 | 9.9 | 9.6 | 9.5 | 9.4 | 9.5 | 10.5 | 10.8 |
| 11.3 | 10.2 | 10.5 | 10.6 | 9.8 | 9.5 | 10.1 | 11.5 | 9.5 | 9.4 | 9.4 | 10 | 10.5 | 10.1 | 9.7 | 9.5 | 9.5 | 9.5 | 10 | 10.8 | 10.4 |
| 10.4 | 11 | 10.7 | 10.1 | 9.4 | 9.4 | 9.7 | 11.3 | 9.4 | 9.4 | 9.4 | 10.6 | 10.7 | 10 | 9.5 | 9.4 | 9.5 | 9.7 | 10.6 | 10.7 | 10 |
| 9.6 | 11 | 10.4 | 9.7 | 9.4 | 9.4 | 9.5 | 11.1 | 9.4 | 9.4 | 9.4 | 11.1 | 10.6 | 9.9 | 9.5 | 9.4 | 9.7 | 10.3 | 11 | 10.5 | 0.7 |
| 9.4 | 10.4 | 10 | 9.6 | 9.4 | 9.4 | 9.4 | 10.7 | 9.4 | 9.4 | 9.4 | 11 | 10.4 | 9.8 | 9.5 | 9.5 | 10.3 | 11 | 10.9 | 10 | 9.6 |
| 9.4 | 9.9 | 9.7 | 9.5 | 9.4 | 9.4 | 9.4 | 10.5 | 9.4 | 9.4 | 9.4 | 10.7 | 10 | 9.6 | 9.5 | 9.5 | 10.9 | 11.4 | 10.5 | 9.7 | 9.5 |
| 9.4 | 9.4 | 9.4 | 9.5 | 9.4 | 9.4 | 9.4 | 10 | 9.4 | 9.3 | 9.3 | 10 | 9.7 | 9.5 | 9.4 | 9.5 | 11.3 | 11.1 | 10 | 9.5 | 9.4 |
| 9.4 | 9.4 | 9.4 | 9.5 | 9.4 | 9.4 | 9.4 | 9.8 | 9.4 | 9.4 | 9.4 | 9.6 | 9.5 | 9.5 | 9.5 | 9.5 | 11.4 | 10.5 | 9.6 | 9.5 | 9.4 |
| 9.4 | 9.4 | 9.4 | 9.4 | 9.4 | 9.4 | 9.4 | 9.4 | 9.4 | 9.4 | 9.4 | 9.4 | 9.4 | 9.4 | 9.4 | 9.5 | 11 | 9.8 | 9.5 | 9.4 | 9.4 |
| 9.4 | 9.4 | 9.3 | 9.4 | 9.4 | 9.4 | 9.4 | 9.2 | 9.4 | 9.4 | 9.4 | 9.3 | 9.4 | 9.4 | 9.4 | 9.5 | 10.4 | 9.5 | 9.4 | 9.4 | 9.4 |
| 9.4 | 9.4 | 9.3 | 9.4 | 9.4 | 9.4 | 9.4 | 9.1 | 9.4 | 9.4 | 9.4 | 9.3 | 9.4 | 9.4 | 9.4 | 9.6 | 9.7 | 9.4 | 9.4 | 9.4 | 9.4 |
| 9.3 | 9.4 | 9.4 | 9.4 | 9.4 | 9.4 | 9.4 | 9 | 9.4 | 9.4 | 9.4 | 9.3 | 9.4 | 9.4 | 9.4 | 9.7 | 9.4 | 9.4 | 9.4 | 9.4 | 9.4 |
| 9.4 | 9.4 | 9.4 | 9.4 | 9.4 | 9.4 | 9.4 | 9 | 9.4 | 9.4 | 9.4 | 9.3 | 9.4 | 9.4 | 9.4 | 9.7 | 9.4 | 9.4 | 9.4 | 9.4 | 9.4 |
| 9.4 | 9.4 | 9.4 | 9.4 | 9.4 | 9.4 | 9.4 | 9 | 9.4 | 9.4 | 9.4 | 9.3 | 9.4 | 9.4 | 9.4 | 9.7 | 9.4 | 9.4 | 9.4 | 9.4 | 9.4 |
| 17 | 17 | 17 | 17 | 17 | 17 | 17 | 16.6 | 17 | 16.9 | 16.9 | 17 | 17 | 17 | 17 | 16.9 | 16.8 | 16.9 | 17 | 17 | 17 |